ASPHALT MIXTURES MODIFIED BY AMAZONIAN BIOCHAR

Alemar Pereira Torres[1], Rayanne Oliveira de Araújo[2], Newton Paulo de Souza Falcão[2], Carlos Eduardo Neves de Castro[1] and Consuelo Alves da Frota[1]
[1]Geotechnics Research Group – Geotec, Federal University of Amazonas, General Rodrigo Octavio Jordão Ramos Avenue, 1200, Coroado I, 69067 005, Manaus, Amazonas, Brazil
rayannearaujo20@gmail.com
nfalcao@inpa.gov.br
[2]National Amazon Research Institute – INPA, André Araújo Avenue, 2936, Petrópolis, 69067 375, Manaus, Amazonas, Brazil
eng.alemar@hotmail.com
carlosnvscastro@gmail.com
cafrota@ufam.edu.br

ABSTRACT

Alternative materials, notably those that help the sustainable development, result in great environmental, social, and economic benefits. In this respect, biochar is a promising option in geotechnical problems, such as in improving the mechanical properties of asphalt binder. The present research performs an experimental and theoretical rheological study on the asphalt concrete added with biochar from the Brazil nut hedgehog biomass, using the four-point bending test and the Huet-Sayegh rheological model. Two types of hot asphalt composites were studied: i) a reference mixture without biochar (CA+0%BC); and ii) a modified asphalt binder with the addition of 3% of biochar (CA+3% BC). It is observed that for these asphalt mixtures the dynamic modulus decreases with the increasing of the temperature and frequency, as well as the phase angle behaves inversely proportional to the frequency. The behavior of the master curve and at the reference temperature of 40°C point out that the biochar mixed into asphalt cement produces great stability for CA at high temperatures. The values of the dynamic modulus determined from the Huet-Sayegh model and experimental showed excellent approximations for both composites asphalt.

KEYWORDS: *Asphalt Mixture, Amazonian Biochar, Four-point bending test, Huet-Sayegh.*

I. INTRODUCTION

The Industrial Revolution transformed the socio-economic life of humanity and drove the advancement of science and technology, linking human needs to technological dependence. Although these changes have resulted in greater comfort in daily activities, there have been implications related to climate change, water, and soil pollution, waste generation, fossil fuel depletion, food shortages, among others [1]. In this sense, through alternative materials, sustainable development arises with the aim of mitigating these issues and their unfolding in the social, economic, and environmental spheres. In this context, biochar appears as a promising component given its ability to solve multiple problems simultaneously [1].

Biochar is a solid material, by-product of organic matter pyrolysis (biomass) under little or no oxygen, characterized by its porous structure rich in carbon, high cation exchange capacity, and high specific surface area [1-4]. The laboratory process of obtaining it can mainly take place by fast pyrolysis (300° C – 1500 ° C), slow (350° C – 800° C), or gasification (700° C – 1500°C) [5], from any type of organic matter, with preference for those available in abundance [1-4].

Although the improvement of soil agronomic properties represents the primary use of biochar [5-6] due to its high specific surface area and porosity, it has found other applications in engineering, such as fuel catalysts as syngas and biodiesel, and adsorbent of pollutants in water and air [7-12]. As a building material, adding it to cementitious composites improves mechanical properties such as tensile and compressive strength [7-12]. In Geotechnics, biochar can decrease plasticity and increase parameters such as CBR, unconfined compressive strength (UCS), and shear strength of cohesive soils [13-18].

Given the versatility of this material, its effects are also evaluated in the composition of asphalt surface layer, both as a binder modifier [19-23] and as a mineral aggregate [21, 24-26]. From the physical perspective, studies indicate that adding biochar to the asphalt binder decreases the penetration, increases the softening point, reduces the volatilization of light asphalt components, and decreases sensitivity to high temperatures and aging [19-23]. Concerning to the mechanical performance of asphalt mixtures, researches indicate that biochar increases the Marshall stability, rutting, and fracture resistance after aging, as well as attenuates the susceptibility of asphalt concrete to moisture and high temperatures [26-28].

As for the rheological behavior, [29] compared asphalt compositions with modified binders by the addition of 5% and 10% of biochar from two different obtaining methods, fast pyrolysis, and slow pyrolysis. The authors also evaluated the formulations for short-term (4h) and long-term (120h) aging, pre-conditioning the specimens at 135° C and 85° C, respectively. In their work, they associated the frequency-temperature pair as performance indicators for thermal cracking (–10° C and 25Hz), fatigue cracking (21.1 °C and 10 Hz), and rutting (37.8 °C and 0.1 Hz). As a result, the samples submitted to short-term aging suggest that 5% addition and slow pyrolysis promote better resistance to thermal cracking, while the insertion of 10% and slow pyrolysis improves the coating performance against fatigue and cracking. Regarding rutting, the control mixtures, followed by those modified with 5% biochar and fast pyrolysis, showed better performance. As for long-term aging, the composition containing 10% modifier and slow pyrolysis suggests improvements regarding thermal and fatigue cracking. Rutting indicated the control mixture as the one with the best result, followed by the mixture containing 5% biochar and slow pyrolysis.

It is important to highlight that the literature is scarce relating to works that discuss rheological behavior of asphalt concretes with biochar and, although the rheology of asphalt mixtures is still far from practical applications aimed at design methodologies [30], its viscoelastic mechanical properties and inherent peculiarities cannot be neglected, under penalty of significant overestimation or underestimation of design parameters, given that, when disregarding the mechanical response of an asphalt mix to time and loading frequency dependence, it is possible to overestimate or minimize the thickness of the coating, depending on weather conditions and traffic volume [30].

The present study proposes a rheological analysis of experimental and theoretical character in asphalt concrete added with biochar from the Brazil nut hedgehog biomass (*Bertholletia Excelsa*), through the four-point bending test and the Huet-Sayegh rheological model. Section 1 presents the introduction of this article with a brief literature review on the topic. Section 2 describes the theoretical and experimental methodology of this work. In section 3, the chemical profile of biochar is analyzed and the experimental results of the four-point bending test are discussed and compared with the values predicted by the Huet-Sayegh model for asphalt mixtures. Section 4 describes the conclusions and recommendations regarding the work developed.

II. METHODOLOGY

2.1. Theoretical background

In Figure 1 we present the Huet-Sayegh theoretical model [31-32] used in the analysis of the results presented here. It consists of two parallel branches. The left branch is formed by a set of two dashpots named k and h and a spring of elastic constant $E_\infty - E_0$ arranged in series. This branch is in parallel with the right branch, consisting of a single spring of elastic constant E_0. The two model branches attest that the total stress is given by the sum of the stresses in each branch (Equation 1), and the total strain is equal to the strains in each branch (Equation 2). These strains are functions of the respective stresses and strains of the components in each branch.

$$\sigma = \sigma_L + \sigma_R \quad (1)$$

$$\varepsilon_L = \varepsilon_R = \varepsilon, \quad (2)$$

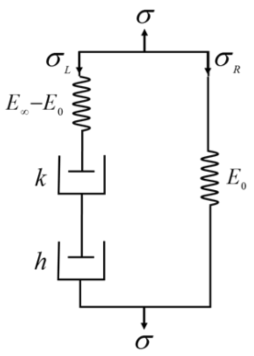

Figure 1. Huet-Sayegh model

where σ (ε) is the total stress (strain) and σ_R (ε_R) and σ_L (ε_L) are the stresses (strains) of the right (R) and left (L) side, respectively. The stresses on the dashpots, according to Huang's definition [33], are given by Equation 3, where *i* is the complex unit, ω = 2π*f* (*f* is the frequency), η is the viscosity, α is a representative variable of the parabolic dashpot, and τ is the relaxation time,

$$\sigma_\alpha = \frac{\eta}{\tau}(i\omega\tau)^\alpha \varepsilon_a. \quad (3)$$

From Eqs. 1-3 and after some algebra, the dynamics modulus E^* of the model represented by Figure 1 is written as

$$E^* = E_0 + \frac{E_\infty - E_0}{1+\delta(i\omega\tau)^{-k}+\delta(i\omega\tau)^{-h}}, (4)$$

where $\delta = \frac{\tau}{\eta}(E_\infty - E_0)$, E_∞ is the dynamics modulus value when frequency tends to infinity, E_0 is the initial dynamic modulus, the δ parameter is a dimensionless constant, h and k are parabolic exponents on the premise of $1 > h > k > 0$, τ is the characteristic time and ω is the angular velocity [31-32].

Equation 4 can be rearranged and take the form of Equation 5 [31],

$$E^* = E_0 + \frac{(E_\infty - E_0)}{A^2+B^2}A + \ i\frac{(E_\infty - E_0)}{A^2+B^2}B, \quad (5)$$

with A and B written as

$$A = 1 + \frac{\delta \cos\left(\frac{k\pi}{2}\right)}{(2\pi f\times\tau)^k} + \frac{\cos\left(\frac{h\pi}{2}\right)}{(2\pi f\times\tau)^h} \quad (6)$$

$$B = \frac{\delta\, sen\left(\frac{k\pi}{2}\right)}{(2\pi f\times\tau)^k} + \frac{sen\left(\frac{h\pi}{2}\right)}{(2\pi f\times\tau)^h}. \quad (7)$$

Rewritten Eq. 5 in its real and imaginary parts, E_1 and E_2, respectively, we obtain

$$E^* = E_1 + iE_2, \ (8)$$

where

$$E_1 = E_0 + \frac{(E_\infty - E_0)}{A^2+B^2}A \quad (9)$$

$$E_2 = \frac{(E_\infty - E_0)}{A^2+B^2}B, \ (10)$$

From Eq. (8), the absolute value of the dynamics modulus is written as

$$|E^*| = \sqrt{E_1{}^2 + E_2{}^2}. \qquad (11)$$

2.2. Materials

The mixtures of asphalt concrete type (CA) integrated the traditional materials used in the pavements building, which are: gravel, sand, stone dust, and asphalt binder. Biochar participated as a bio-carbonized material.

The aggregates gravel and stone dust, acquired in the retail trade, were analyzed by granulometry (ABNT-NBR 17054) [34] and, as for the apparent specific gravity (Gsa), it followed the ASTM C127-15 standard [35]. The residual sand was typified by granulometry (ABNT-NBR 17054) [34]. As for the apparent specific gravity (Gsa), the requirements of ASTM C128-22 [36] were followed. Such analyses were performed in the Geotechnical Research Group (GEOTEC) laboratories from the Federal University of Amazonas. The asphalt binder donated to GEOTEC was specified by the usual characterization of the National Agency of Petroleum and Biofuels (ANP) [37], which establishes the specifications of asphalt petroleum cement (APC) marketed in Brazil.

The biochar material, originated from the pyrolysis of Brazil nut hedgehogs, was donated by the Cellulose and Charcoal Laboratory of the Coordination of Forest Products from the National Institute of Research of the Amazon – INPA. After their collection and upon arrival at the laboratory, they were dried in the oven for 72h to remove moisture before being crushed. The powder resulting from the milling was inserted into an alumina crucible for heat treatment at 600°C for 1h, in a tubular oven under nitrogen gas atmosphere and heating ramp rate of 10°C min-1. These samples were analyzed by X-ray diffractograms, scanning electron microscopy, infrared spectroscopy, and thermogravimetry. X-ray diffractograms were obtained by means of a diffractometer, model XRD 6000 Shimadzu®, operating in a scanning range of 5° to 80° and step size of 0.02° in 2θ. In the case of scanning electron microscopy, the Tescan® equipment was used. Such a device is coupled to the energy dispersive spectroscopy (EDS) system, which provided profile determination and elemental mapping of the biochar composition. For studies specific to the functional groups present in the constitution of this bio-carbonized material were used infrared and Fourier-transform infrared spectroscopy (FTIR) with Agilent Cary 630®, and ATR in the region of 4000-650 cm−1. The thermal decomposition profile was investigated in a Shimadzu TG/DTG thermal analyzer, model DTG-60H®. The samples were subjected to heating in a range of 25 to 850°C, under nitrogen gas at 50 mL min-1 and heating rate of 10°C min-1.

2.3. Methods

Two types of hot asphalt mixtures were investigated. The reference dosage (CA+0%BC), and the alternative asphalt concrete (CA+3% BC), taking a modified asphalt binder with 3% biochar. These formulations followed the standardization of the National Department of Transport Infrastructure (DNIT) [38], both in the mineral composition, according to Range C, as determined in the design content.

Once the dosage was defined, the specimens were compacted in beam shape, in the dimensions of 400 mm in length, 64.5 mm in width and 51.0 mm in height. A metallic rectangular box was used for this purpose. Densification was carried out by means of a Bovenau® hydraulic press P3000 with 30 tons capacity. These samples were controlled during and after compaction in accordance with the density, as well as the dosage requirements inherent to asphalt concrete.

Subsequently, the specimens were tested under flexural stress with dynamic loading at 1Hz, 3 Hz, 5 Hz, 10 Hz, and 20 Hz frequencies, and according to the European standard EN 12697-26:2018 [39] recommendations. In concern to the preservation of samples were run strain-controlled tests for a maximum strain amplitude of 50μm/m, as well as repeated tests with 1Hz frequency to verify the limit not higher than 3%.

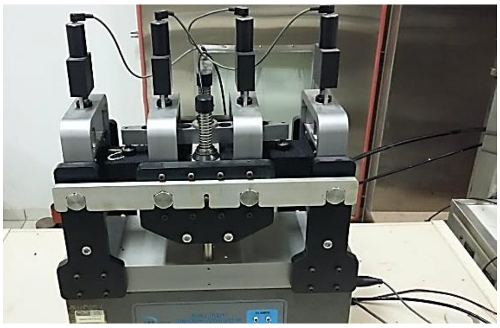

Figure 2. Specimen (beam) on the equipment for four-point bending test.

This experiment was carried out in the Pneumatic Standalone 4 Point Bending apparatus of the IPC Global® belonging to the Geotechnical Research Group – GEOTEC/UFAM. Such equipment has four support points, two internal, located at one third of the ends, which are connected to a pneumatic system that transmits the sinusoidal loading to the specimen (beam). As for the data, the acquisition was through the linear variable differential transformers (LVTD's) connected to a computer, for the purpose of setting up and data storage. Such an apparatus is inserted into a climatic chamber, which makes it possible to study the mechanical properties by varying the temperature. The experiments were carried out at 25ºC for reference temperature and at the 40ºC for design temperature. Figure 2 shows an asphalt concrete specimen inserted for testing in the 4-Point Bending apparatus.

III. RESULTS AND DISCUSSION

3.1. Structural and surface properties of biochar

3.1.1. X-ray diffraction

The heat treatment process of materials with carbon causes dehydration and cleavage of bonds present in the biomass structure, forming amorphous materials similar to polycyclic aromatic rings and randomly oriented. The X-ray diffraction patterns for the sample from the biomass of the Brazil nut hedgehog are recorded in Figure 3. The presence of the amorphous carbon structure was confirmed by the lack of well-defined diffraction peaks and high intensity attributed to the crystal ordering and structure. According to this XRD pattern, it is observed a broad peak of low intensity between 15 and 26°, 2θ, attributed to the (002) plane, which denotes a characteristic of carbon samples with amorphous structure. The sharp peaks for 2θ around 27° and 28° correspond to quartz and calcium phosphate, respectively, which are inorganic components of the biochar structure.

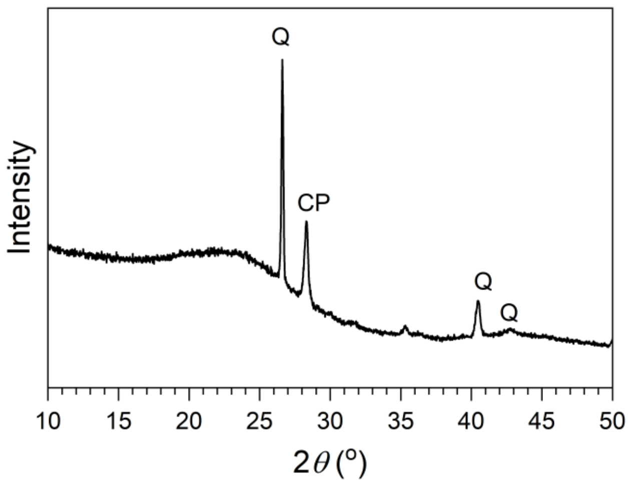

Figure 3. Biochar X-ray diffraction patterns of biochar, obtained by pyrolysis of the Brazil nut hedgehog biomass., where the Q and CP labels represent the peaks from quartz and calcium phosphate, respectively.

The sharp peaks for 2θ around 27° and 28° correspond to quartz and calcium phosphate, respectively, which are inorganic components of the biochar structure.

3.1.2. Scanning Electron Microscopy

The images of biochar, according to scanning electron microscopy, are shown in Figure 4A. This carbonized material at 600°C has amorphous structure, uneven and rough compact surface, as well as the presence of clusters and small fractures. Energy-dispersive X-ray spectroscopy (EDS) (Figure 4b) showed predominant peaks corresponding to the elements carbon and oxygen, which were identified in the concentrations of elements C (88.98% by weight) and O (9.95% by weight) by the elemental map of Figure 4C.

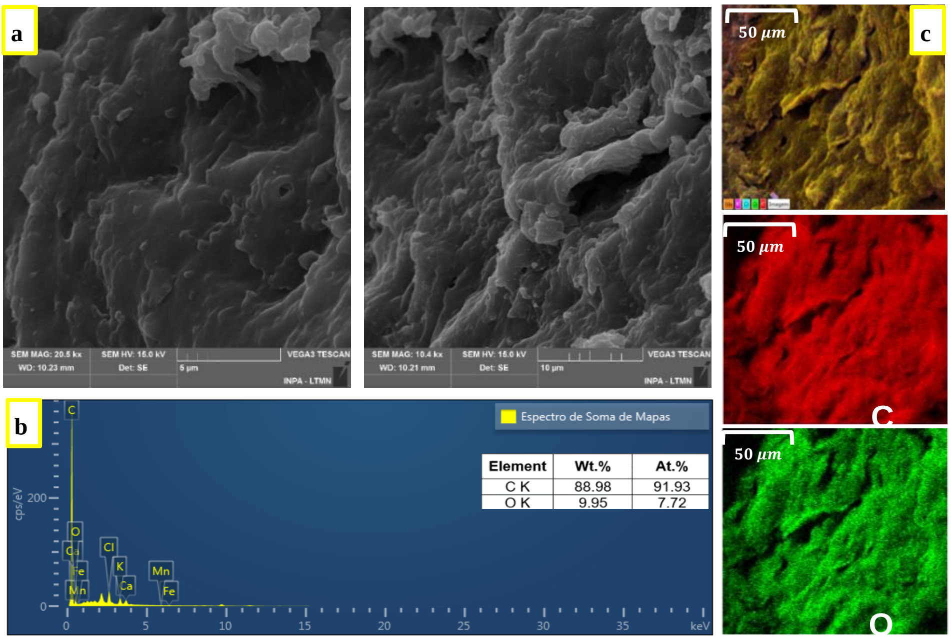

Figure 4. Scanning Electron Microscopy (a), EDS spectrum (b), and EDS elemental map (c)

3.1.3. Scanning Electron Microscopy

The infrared analysis was used to identify the presence of functional groups in the biochar structure. In Figure 5 is shown the infrared transmission spectrum, where absorption bands appear at 2157, 2021 and 1977 cm-1, which are related to the C=C, C—H and C=O bonds, respectively.

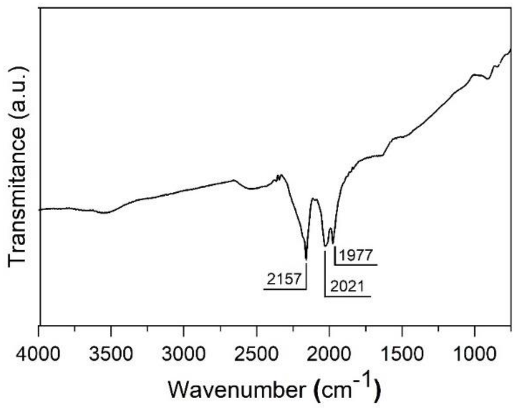

Figure 5. The infrared spectrum of biochar obtained by pyrolysis of the Brazil nut hedgehog biomass.

3.1.4. TG analysis

The thermal stability of the biochar functional groups was estimated from the TG curves, as is shown if Figure 6. Generally, the thermal decomposition of biochar occurs in two stages of mass loss. The first mass loss (1%) is between the initial temperature and 113 °C, which is related to water evaporation and or the partial degradation of light organic compounds. The second mass loss (52%) is between 244 and 832 °C, which is due to the decomposition of the carbon-based material.

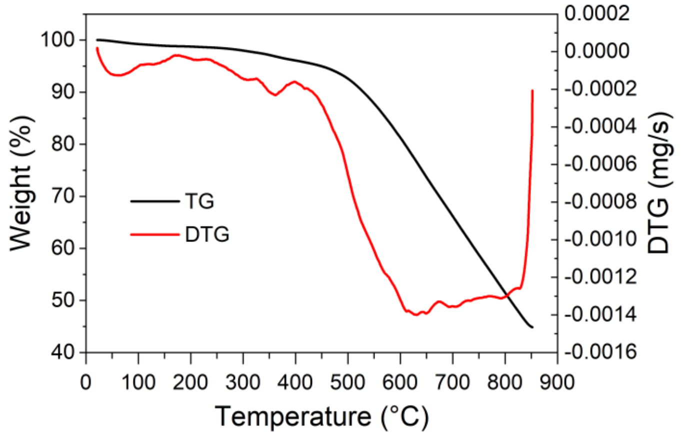

Figure 6. Thermogravimetric (TG) analysis of biochar obtained from Brazil nut hedgehog.

3.2. Properties of aggregates, asphalt cement, and dosage

The granitic materials that integrated the design aggregate structure of the studied asphalt compositions were gravel 1 (9.5 mm to 19 mm) and gravel 0 (4.8 mm to 9.5 mm) as coarse aggregate, a residual sand (4,75 mm passive sieve) as the fine aggregate, and the mineral filler (4,8 mm passive sieve) from stone dust. The apparent specific gravity (Gsa) of these materials resulted in the following values: gravel 1 = 2,63 g/cm³, gravel 0 = 2,61g/cm³, stone dust = 2.57 g/cm³, and sand = 2.60 g/cm³.

The asphalt binder characterization was in accordance with the National Agency of Petroleum and Biofuels (ANP) resolution [37] and the bituminous material was classified as AC 50/70. This specification is important to achieve the experiments aim, especially to ensure the proper viscosity for the suitable mixing and compaction of the asphalt composition.

In summary, the control composition (CA+0%B) consisted of gravel 0 = 28.2%; gravel 1=14.8%; stone dust = 28.2%; sand = 23.8%, and asphalt binder = 5%. Such mineral materials integrated alternative mixture (CA+3%B), as well as the binder modified with 3% biochar. The mentioned formulations presented values around 75.1% and 4.01% referring to voids filled with asphalt (VFA) and air voids (VV) parameters, respectively.

3.3. Structural and surface properties of biochar

3.3.1. Experimental data

The viscoelastic behavior of asphalt concrete beams under four-point bending test can be initially observed by the graphs of Figure 5 for both formulations investigated, that is, the control mix (Figure 5a) and the biochar modified asphalt concrete (Figure 5b).

It is noted the non-alignment of the peaks relative to the curves representing force and displacement as a function of time irrespective of asphalt mixtures [40]. For the composite CA+0%BC (Figure 5a), there is a maximum force value close to 0.03kN and a displacement about 0.04mm. In the CA+3%BC (Figure

5b) formulation, the force and displacement showed peaks of the order of 0.038kN and 0.015mm, respectively.

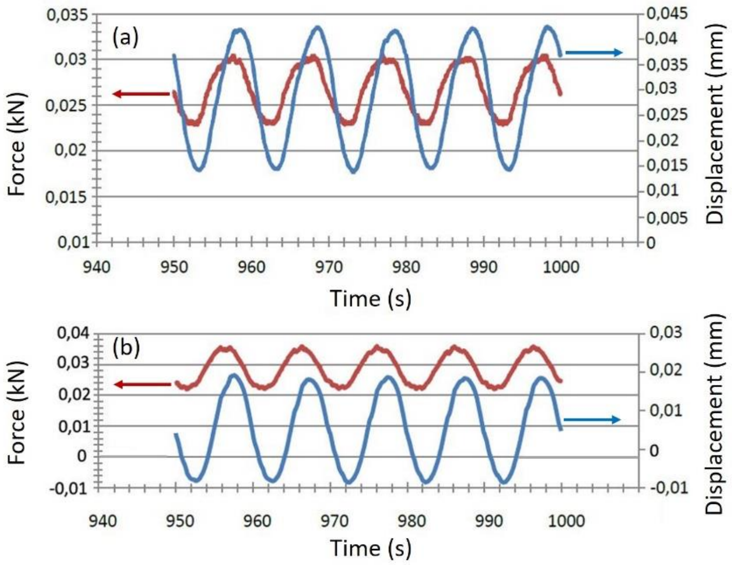

Figure 5. Force and displacement for beams CA+0% BC (a) and CA+3%BC (b)

Figure 6 presents the results of the flexural test as a function of the mechanical parameters, dynamic modulus (Figure 6a) and phase angle (Figure 6b), for the control mixes (CA+0% BC) and the 3% biochar modified mixes (CA+3%BC) evaluated at 25°C and 40°C temperatures.

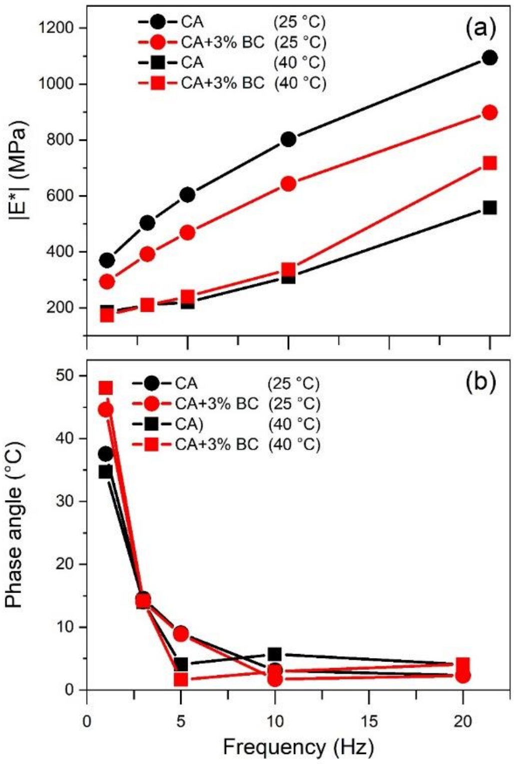

Figure 6. Variation with temperature and frequency: (a) dynamic modulus x (b) phase angle

For both asphalt mixtures (CA+0%BC and CA+3%BC), as expected and verified by the literature [4,41-42], the dynamic modulus value decreased with the increasing of the temperature and increased as there were increases in frequency (Figure 6a).

It is observed that the addition of biochar to the asphalt composite decreased the dynamic modulus for the tested frequencies. On the other hand, it should be noted that when there was an increase in temperature such changes were smaller in the samples made with the additive (CA+3%BC), which may indicate better performance of the modified composition at high temperatures [20]. For example, at the 3Hz frequency, the dynamic modulus of unmodified formulations (CA+0%BC) showed a reduction of 63.5%, while in mixtures with biochar (CA+3%BC) it resulted in 47.5%. It is also noteworthy the response at 20 Hz frequency, in which the modified and unmodified compositions indicated 21.3% and 58.8% decrease, respectively.

In relation to the phase angle (Figure 6b), the results are inversely proportional to the frequency in all cases studied. In particular, the bio-carbonized material (CA+3%BC) had the highest phase angle value at the frequency of 1 Hz at 40°C. On the other hand, at the frequency of 3Hz, the results indicate similarities, regardless of the type of sample and temperature. From 5Hz the temperature is again predominant in the results. In this frequency, there is a decrease with the increase in temperature and growth in the other frequencies (10Hz and 20Hz).

3.3.2. Theoretical-experimental analysis and calibration of the Huet-Sayegh model

The E_∞, E_0, δ, h, k and τ parameters mentioned in item 2 were calibrated, according to [43], by means of sum-of-squares optimization, having as input the results of the experimental dynamic modulus and those calculated by the model.

Therefore, after the iterations, the necessary parameters of the dynamic modulus were obtained from the Huet-Sayegh model, which made possible to construct the master curves at the reference temperature T_{ref} = 40°C (Figure 7a). The results alluding to the values of the parameters for the control composite (CA+0%BC), were: $E_0 = 163.24$; $E_\infty = 4152.55, h = 0.99, k = 0{,}56, \delta = 15.64,$ and $\tau = 7.47E - 03$. In the case of asphalt mixture with addition of the bio-carbonized material (CA+3%BC), the model provided: $E_0 = 126.80$; $E_\infty = 5712.24; h = 0.54; k = 0.54; \delta = 11.49$ and $\tau = 4.41E - 03$.

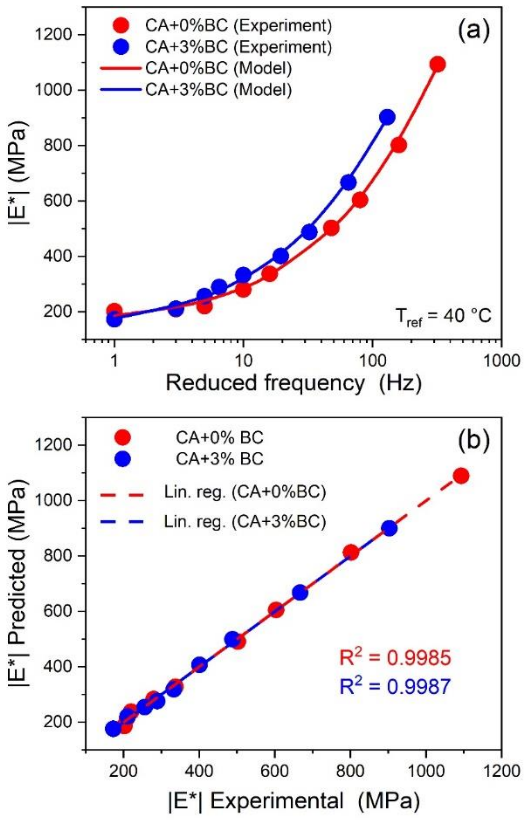

Figure 7. (a) Master curve with theoretical and experimental data and (b) theoretical data x experimental data of the dynamic modulus

The E_∞ parameter, in the Huet-Sayegh model, according to [44], is equivalent to the purely elastic modulus, whose value in the alternative mixture (CA+3%BC) was about 37% higher, relative to the control asphalt composite. In the case of the E_0 parameter, relative to residual resistance at high temperatures [44], relatively close values were obtained in both cases (CA+0%BC and CA+3%BC).

For characteristic time τ, which is a function of temperature [44], a lower value was recorded in formulations modified with biochar (CA+3%BC). The coefficient δ, function of the nature of the bitumen and the granulometric curve (Almeida et al., 2018), decreased when biochar was added to asphalt concrete. Regardless of the composite investigated, the k parameters remained close, while the h parameter decreased with the incorporation of the additive to the asphalt mixture.

In summary, when evaluated individually and at the frequencies studied, the addition of biochar decreased the values of the dynamic modulus (Figure 6a). However, when applying the principle of time-temperature superposition and at the reference temperature of 40°C, the most worrying being the condition of thermosensitivity of the asphalt, it is noted that, in the range of 1 to 10Hz of the reduced frequency, the differences are not very expressive (Figure 7a), and, from there, the modified mixture (CA+3%BC) exhibits better performance compared to the conventional one. This behavior may indicate that the insertion of biochar implied greater stability of the asphalt mixture at high temperatures, as observed in [20], whose study demonstrated an improvement in the thermal sensitivity of a binder modified with biochar, from vegetable straws in contents of 5% to 15%, including at low frequencies.

In the case of the model's ability to predict the value of the dynamic modulus, when comparing the theoretical and experimental results (Figure 7b), it is possible to observe excellent approximations of both mixtures (CA+0%BC and CA+3%BC), as verified by the coefficients of determination R^2 of the order of 99.8%.

Finally, it is emphasized that, in the asphalt mixture, there are interactions of several components, such as aggregates, which will also dictate the mechanical behavior. In addition, the physicochemical properties of biochar depend on the raw material that originated it and on the preparation conditions [45-46]. Therefore, the best results can occur in different percentages, depending on the biomass used in the production of biochar. The present work is an initial study on the behavior of this bio-carbonized material stemming from the Brazil nut hedgehog and, therefore, other percentages of addition should be investigated.

IV. CONCLUSIONS

The biomass of the Brazil nut hedgehog presented a structure with the amorphous carbon, quartz and calcium phosphate as inorganic components. It was also identified in this material bonds of the type C=C, C—H and C=O. The mass loss of biochar occurs in two stages, between the initial temperature and 113°C, and between 244 and 832°. Two asphalt mixtures were investigated: the control composition (CA+0%BC), containing gravel 0 = 28.2%, gravel 1 =14.8%, stone dust = 28.2%, sand = 23.8%, and asphalt binder = 5%, and the alternative mixture formed by adding 3% of biochar to the control composition (CA+3%BC). The experimental data for asphalt mixtures CA+0%BC (CA+3%BC) showed maximum force values and displacement of the 0.03kN and 0.04mm (0.038kN and 0.015mm), respectively. For both composites the dynamic modulus value decreased with the increasing of temperature and frequency. It noted also that when occurred an increase in temperature such changes were smaller in the samples with the additive (CA+3%BC). In the case of phase angle values, they were inversely proportional to the frequency for the two formulations. From the master curve and at the reference temperature of 40°C, it is observed that for reduced frequency of 10Hz, the mixture CA+3%BC showed better performance compared to composite CA+0%BC. This behavior indicated that the presence of the biochar presented greater stability of asphalt formulation at high temperatures. For both mixtures (CA+0%BC and CA+3%BC), there is an excellent concordance of the dynamics moduli between the Huet-Sayegh model and the experimental results.

REFERENCES

[1]. Kumar, A., & Bhattacharya, T. (2021). Biochar: a sustainable solution. Environment, Development and Sustainability, 23, 6642-6680.

[2]. Xie, Y., Wang, L., Li, H., Westholm, L. J., Carvalho, L., Thorin, E., ... & Skreiberg, Ø. (2022). A critical review on production, modification and utilization of biochar. Journal of Analytical and Applied Pyrolysis, 161, 105405.

[3]. Zhou, Y., Qin, S., Verma, S., Sar, T., Sarsaiya, S., Ravindran, B., ... & Awasthi, M. K. (2021). Production and beneficial impact of biochar for environmental application: A comprehensive review. Bioresource Technology, 337, 125451.

[4]. Wang, J., & Wang, S. (2019). Preparation, modification and environmental application of biochar: A review. Journal of Cleaner Production, 227, 1002-1022.

[5]. Igalavithana, A. D., Mandal, S., Niazi, N. K., Vithanage, M., Parikh, S. J., Mukome, F. N., ... & Ok, Y. S. (2017). Advances and future directions of biochar characterization methods and applications. Critical reviews in environmental science and technology, 47(23), 2275-2330.

[6]. Ajayi, A. E., & Rainer, H. O. R. N. (2017). Biochar-induced changes in soil resilience: effects of soil texture and biochar dosage. Pedosphere, 27(2), 236-247.

[7]. Qian, K., Kumar, A., Zhang, H., Bellmer, D., & Huhnke, R. (2015). Recent advances in utilization of biochar. Renewable and Sustainable Energy Reviews, 42, 1055-1064.

[8]. Cha, J. S., Park, S. H., Jung, S. C., Ryu, C., Jeon, J. K., Shin, M. C., & Park, Y. K. (2016). Production and utilization of biochar: A review. Journal of Industrial and Engineering Chemistry, 40, 1-15.

[9]. Wani, I., Ramola, S., Garg, A., & Kushvaha, V. (2021). Critical review of biochar applications in geoengineering infrastructure: moving beyond agricultural and environmental perspectives. Biomass Conversion and Biorefinery, 1-29.

[10]. Leng, L., Xiong, Q., Yang, L., Li, H., Zhou, Y., Zhang, W., ... & Huang, H. (2021). An overview on engineering the surface area and porosity of biochar. Science of the total Environment, 763, 144204.

[11]. Lopes, R. P., & Astruc, D. (2021). Biochar as a support for nanocatalysts and other reagents: Recent advances and applications. Coordination Chemistry Reviews, 426, 213585.

[12]. Legan, M., Gotvajn, A. Ž., & Zupan, K. (2022). Potential of biochar use in building materials. Journal of Environmental Management, 309, 114704.

[13]. GuhaRay, A., Guoxiong, M., Sarkar, A., Bordoloi, S., Garg, A., & Pattanayak, S. (2019). Geotechnical and chemical characterization of expansive clayey soil amended by biochar derived from invasive weed species Prosopis juliflora. Innovative Infrastructure Solutions, 4, 1-10.

[14]. Kumar, H., Huang, S., Mei, G., & Garg, A. (2021). Influence of feedstock type and particle size on efficiency of biochar in improving tensile crack resistance and shear strength in lean clayey soil. International Journal of Damage Mechanics, 30(4), 646-661.

[15]. Gonzalez, J., Sargent, P., & Ennis, C. (2021). Sewage treatment sludge biochar activated blast furnace slag as a low carbon binder for soft soil stabilisation. Journal of Cleaner Production, 311, 127553.

[16]. Michelon, W., Nienov, F. A., Knoblauch, P. M., Regalin Júnior, G., Luvizão, G., Málaga, P. R., ... & Shah, M. P. (2022). Biochar produced from eggshell waste applied for removal of water-polluting substances and clayey soil stabilization: an environmental friendly application. Biomass Conversion and Biorefinery, 1-12.

[17]. Wani, I., Kushvaha, V., Garg, A., Kumar, R., Naik, S., & Sharma, P. (2022). Review on effect of biochar on soil strength: towards exploring usage of biochar in geo-engineering infrastructure. Biomass Conversion and Biorefinery, 1-32.

[18]. Ritter, S., Paniagua, P., & Cornelissen, G. (2023). Biochar in Quick Clay Stabilization: Reducing Carbon Footprint and Improving Shear Strength. In Geo-Congress 2023 (pp. 15-24).

[19]. Dong, W., Ma, F., Li, C., Fu, Z., Huang, Y., & Liu, J. (2020). Evaluation of anti-aging performance of biochar modified asphalt binder. Coatings, 10(11), 1037.

[20]. Ma, F., Dai, J., Fu, Z., Li, C., Wen, Y., Jia, M., ... & Shi, K. (2022). Biochar for asphalt modification: A case of high-temperature properties improvement. Science of The Total Environment, 804, 150194.

[21]. Rondón-Quintana, H. A., Reyes-Lizcano, F. A., Chaves-Pabón, S. B., Bastidas-Martínez, J. G., & Zafra-Mejía, C. A. (2022). Use of Biochar in Asphalts. Sustainability, 14(8), 4745.

[22]. Zhang, R., Wang, H., Ji, J., & Wang, H. (2022). Viscoelastic Properties, Rutting Resistance, and Fatigue Resistance of Waste Wood-Based Biochar-Modified Asphalt. Coatings, 12(1), 89.

[23]. Martínez-Toledo, C., Valdés-Vidal, G., Calabi-Floody, A., González, M. E., & Reyes-Ortiz, O. (2022). Effect of Biochar from Oat Hulls on the Physical Properties of Asphalt Binder. Materials, 15(19), 7000.

[24]. Wu, Y., Cao, P., Shi, F., Liu, K., Wang, X., Leng, Z., ... & Zhou, C. (2020). Modeling of the complex modulus of asphalt mastic with biochar filler based on the homogenization and random aggregate distribution methods. Advances in Materials Science and Engineering, 2020, 1-12.

[25]. Yaro, N. S. A., Sutanto, M. H., Habib, N. Z., Usman, A., Kaura, J. M., Murana, A. A., ... & Jagaba, A. H. (2023). A Comprehensive Review of Biochar Utilization for Low-Carbon Flexible Asphalt Pavements. Sustainability, 15(8), 6729.

[26]. Zhao, S., Huang, B., Shu, X., & Ye, P. (2014). Laboratory investigation of biochar-modified asphalt mixture. Transportation Research Record, 2445(1), 56-63.

[27]. Rengarasu, T. M., Priyankara, S. A. D., Bandara, W. M., & Jegatheesan, N. (2022). Use of Carbonized Rice Husk and Bio-char as Binder Modifiers in Hot Mix Asphalt. ENGINEER, 55(04), 61-70.

[28]. Saadeh, S., Al-Zubi, Y., Katawal, P., Zaatarah, B., & Fini, E. (2023). Biochar effects on the performance of conventional and rubberized HMA. Road Materials and Pavement Design, 24(1), 156-172.

[29]. Owolabi, O.O. (2019). The effect of biochar in asphalt mixtures. Master's thesis. University of New Brunswick, CA.

[30]. Hajikarimi, P., & Nejad, F. M. (2021). Applications of viscoelasticity: Bituminous materials characterization and modeling. Elsevier.

[31]. Tai Nguyen, H. T., Nguyen, D. L., Tran, V. T., & Nguyen, M. L. (2022). Finite element implementation of Huet-Sayegh and 2S2P1D models for analysis of asphalt pavement structures in time domain. Road Materials and Pavement Design, 23(1), 22-46.

[32]. Xu, Q., & Solaimanian, M. (2009). Modelling linear viscoelastic properties of asphalt concrete by the Huet–Sayegh model. International Journal of Pavement Engineering, 10(6), 401-422.

[33]. Huang, Yang H. (2004). Pavement Analysis and Design. Estados Unidos: Pearson, 2004. 2 ed. 775 p.

[34]. Associação Brasileira de Normas Técnicas – ABNT. (2022). NBR 17054: Agregados - Determinação da composição granulométrica - Método de ensaio. Rio de Janeiro, RJ, Brasil.

[35]. American Society for Testing and Materials – ASTM. (2024). ASTM C127-15: Standard Test Method for Relative Density (Specific Gravity) and Absorption of Coarse Aggregate.

[36]. American Society for Testing and Materials – ASTM. (2023). ASTM C128-22: Standard Test Method for Relative Density (Specific Gravity) and Absorption of Fine Aggregate

[37]. Brasil. (2022). Resolução ANP Nº 897, de 18 de novembro de 2022. Dispõe sobre as especificações dos asfaltos e dos aditivos asfálticos de reciclagem para misturas à quente, e suas regras de comercialização em todo o território nacional. Agência Nacional do Petróleo, Gás Natural e Biocombustíveis. Brasília, DF, Brasil.

[38]. Departamento Nacional de Infraestrutura de Transportes - DNIT. (2006). DNIT 031/2006: Pavimentos flexíveis – concreto asfáltico – especificação do serviço. Rio de Janeiro, RJ, Brasil.

[39]. European Committee for Standardization. (2023). EN 12697-26:2018+A1:2022: Bituminous Mixtures - Test Methods for Hot Mix Asphalt - Part 26: Stiffness.

[40]. Mackiewicz, P., & Szydło, A. (2019). Viscoelastic parameters of asphalt mixtures identified in static and dynamic tests. Materials, 12(13), 2084.

[41]. Jamshidi, A., White, G., & Hosseinpour, M. (2021). Revisiting the correlation between the dynamic modulus and the flexural modulus of hot mixture asphalt. Construction and Building Materials, 296, 123697

[42]. Ai, X., Cao, J., Feng, D., Gao, L., Hu, W., & Yi, J. (2022). Performance evaluation of recycled asphalt mixtures with various percentages of RAP from the rotary decomposition process. Construction and Building Materials, 321, 126406.

[43]. Gkyrtis, K., Loizos, A., & Plati, C. (2021). A mechanistic framework for field response assessment of asphalt pavements. International Journal of Pavement Research and Technology, 14(2), 174-185.

[44]. Nilsson, R. N.; Hopman, P. C.; Isacsson, U. (2002). Influence of different rheological models on predicted pavement responses in flexible pavements. Road Materials and Pavement Design, 3(2), 117-149.

[45]. Panwar, N. L., & Pawar, A. (2020). Influence of activation conditions on the physicochemical properties of activated biochar: A review. Biomass Conversion and Biorefinery, 1-23.

[46]. Araujo, R. O., Ribeiro, F. C., Santos, V. O., Lima, V. M., Santos, J. L., Vilaça, J. E., ... & de Souza, L. K. (2021). Renewable energy from biomass: an overview of the Amazon region. BioEnergy Research, 1-16.

AUTHORS

Alemar Pereira Torres is a Civil Engineer (2011) and Masters in Science and Materials Engineering with an emphasis on road paving from the Federal University of Amazonas (2018). He has experience in higher education, projects, planning and execution of civil works in general, such as: buildings, special works of art, urban infrastructure, and so on.

Rayanne Oliveira de Araújo has a bachelor's degree in Chemistry from the Federal University of Amazonas (2013). Graduated in Chemistry from Faculdade Metropolitana de Manaus (2023). Master (2018) and PhD (2022) in Chemistry from the Federal University of Amazonas, developing research at the Fuel Research and Testing Laboratory. Currently, she works on the following topics: synthesis of heterogeneous sulfonated catalysts for application in biofuels and chemicals; study of the characterization and application of biomass from the Amazon; carbon materials applied as controlled release fertilizers.

Consuelo Alves da Frota is a Full Professor at the Faculty of Technology (FT) of the Federal University of Amazonas (UFAM), working in the field of Civil Engineering, with an emphasis on Geotechnical investigations. She has a Postdoctoral degree in Geotechnical Engineering (University of Tennessee, EUA, 1992). PhD in Transport Engineering (USP, 1985). Master in Transport Engineering (USP, 1981). Founder and former ex-Head of the Soil Mechanics Laboratory (FT/UFAM). Founder and ex-Head of the Paving Laboratory (FT/UFAM). Co-founder and first Coordinator of the Postgraduate Program in Resource Engineering of the Amazon (PPGENGRAM), currently belongs to the Postgraduate Program in Materials Science and Engineering (PPGCEM) at the Federal University of Amazonas (UFAM). Founder and leader of the Geotechnical Research Group (GEOTEC) at the Federal University of Amazonas (UFAM). Develops research into technological innovation in the search for new materials for civil construction, notably for use in paving.